Dynamics of α-CH Deprotonation and α-Desilylation Reactions of Tertiary Amine Cation Radicals

Xiaoming Zhang,[†] Syun-Ru Yeh,[†] Seok Hong,[†,‡] Mauro Freccero,[‡] Angelo Albini,[‡] Daniel E. Falvey,[†] and Patrick S. Mariano*,[†]

Contribution from the Department of Chemistry and Biochemistry, University of Maryland, College Park, Maryland 20742, Department of Organic Chemistry, University of Pavia, Pavia, Italy I-27100, and Institute of Organic Chemistry, University of Torino, Torino, Italy I-10125

Received December 31, 1993[⊕]

Abstract: Time-resolved laser spectroscopy has been used to generate and characterize a series of tertiary amine cation radicals and to determine the rates of their α-CH deprotonation and α-desilylation reactions with bases and silophiles. Laser excitation (308 nm) of a 60:40 MeOH:MeCN solution of $PhNMe_2$ (DMA) and 1,4-dicyanobenzene (DCB) promotes SET-induced formation of the DMA cation radical (460 nm) and DCB anion radical (340 nm), which undergo decay by back electron transfer at nearly equal rates and with respective second-order rate constants of 1.1×10^{10} and 1.3×10^{10} M^{-1} s^{-1} (25 °C). The decay rate is lowered (*ca.* 4-fold) by the inclusion of salts (*ca.* 0.1 M) such as nBu_4NClO_4, $LiClO_4$, nBu_4NCl, nBu_4NBF_4, and $nBu_4NO_3SCF_3$ in MeOH–MeCN and by changing the solvent from MeCN to MeOH and to EtOH. The cation radical of $PhNMeCH_2(TMS)$ (480 nm) and the simultaneously generated DCB anion radical undergo second order decay in MeCN with respective rate constants of 1.2×10^{10} and 9.9×10^9 M^{-1} s^{-1} (25 °C). The silylamine cation radical decay rate was found to be governed by the concentration of silophiles (MeOH, H_2O, and nBu_4NF) in MeCN solutions. The observations are consistent with a silophile-induced desilylation process with second-order rate constants of 8.9×10^5 (MeOH), 1.27×10^6 (H_2O), and 3.1×10^9 M^{-1} s^{-1} (nBu_4NF). The rate of DMA cation radical decay is a function of base concentration. Both nBu_4NOAc and $nBu_4NO_2CCF_3$ react with the DMA cation radical (in 60:40 MeOH:MeCN containing 0.1 M nBu_4NClO_4) with second-order rate constants for α-CH deprotonation of 3.1×10^5 and 8×10^4 M^{-1} s^{-1} (25 °C), respectively. Measurements with $PhN(CD_3)_2$ and nBu_4NOAc gave a k_H/k_D for α-CH deprotonation of 3.6 (60:40 MeOH:MeCN, 25 °C). Para-substituents have a pronounced effect on the rate of α-CH deprotonation by nBu_4NOAc; second-order rate constants of 2.3×10^4, 1.1×10^5, and 2.5×10^6 M^{-1} s^{-1} were determined for the *p*-$OMeC_6H_4NMe_2$, *p*-$MeC_6H_4NMe_2$ and *p*-$CF_3C_6H_4NMe_2$ cation radicals. Studies with Ph_2NMe demonstrated that its cation radical (645 nm) can be generated by SET to DCB and that its decay through α-CH deprotonation by nBu_4NOAc has a second-order rate constant of 9.5×10^5 M^{-1} s^{-1} and a k_H/k_D value of 2.8 (25:75 MeOH:MeCN, 25 °C). Finally, the effects of α-substituents on the rates of nBu_4NOAc-induced α-CH deprotonation of tertiary amine cation radicals were evaluated by use of the amines $Ph_2NCHR_1R_2$. The second-order rate constants (25 °C, 25:75 MeOH:MeCN) are 2.3×10^5 (R_1 = Me, R_2 = H), 1.7×10^5 (R_1 = R_2 = Me), 3.2×10^6 (R_1 = Ph, R_2 = H), 2.6×10^6 (R_1 = CH=CH_2, R_2 = H), and 7.0×10^7 M^{-1} s^{-1} (R_1 = C≡CH, R_2 = H).

Introduction

Interest continues to expand in the area of electron-transfer (SET) photochemistry. The overlapping issues of reaction mechanism and synthetic potential[2] have stimulated efforts to gain detailed information about the individual steps involved in the overall SET-reaction pathways and to develop methods to successfully predict new and efficient photochemical processes. Much attention has been given to understanding the properties of ion radicals owing to the key role these intermediates play in SET-induced photochemical reactions. In general, ion radicals formed by SET between neutral donors and acceptors can either decay by back electron transfer to produce ground-state reactants or undergo chemical reaction to produce radical or ionic precursors of photoproducts. Consequently, the efficiencies (chemical and quantum) and nature of SET-photochemical processes are governed to a large extent by the rates and types of reaction pathways open to the ion radical intermediates. Owing to this, it is understandable why much attention has been focused on assessing ion radical reactivity. A number of photochemical[2,3] and electrochemical[4] studies have been designed to gain information about this issue through the analysis and interpretation of product distributions arising from processes proceeding *via* the intermediacy of charged radicals. In contrast, only a few investigations have employed direct methods to determine ion radical reaction rates and to evaluate how they are influenced by structural, substituent, and medium variations.[5]

In early efforts[6] concentrating on the SET photochemistry of iminium cation–neutral donor pairs, indirect methods based on product distribution and quantum efficiency data were used by one of us to define the unique and high chemical reactivity of allyl- and benzylsilane cation radicals.[3,7] In more recent

† University of Maryland.
‡ Universities of Pavia and Torino.
⊕ Abstract published in *Advance ACS Abstracts,* May 1, 1994.
(1) Permanent address: Department of Chemistry, Kungnam National University, Masan, Korea.
(2) (a) Fox, M. A.; Chanon, M. *Photoinduced Electron Transfer*; Elsevier: New York, 1988. (b) Mariano, P. S. *Advances in Electron Transfer Chemistry*; JAI Press: Greenwich, CT, 1991. (c) Fox, M. A. *Advances in Photochemistry*; Volmman, D. H., Hammond, G. S., Gollnick, K., Eds.; Wiley: New York, 1986; Vol. 13, p 295.
(3) d'Alessandro, N.; Albini, A.; Mariano, P. S. *J. Org. Chem.* **1993**, *58*, 937.
(4) See, for instance: Mann, C. K.; Barnes, K. K. *Electrochemical Reactions in Nonaqueous Systems*; Marcel Dekker: New York, 1970. Yoshida, K. *Electrooxidation in Organic Chemistry*; Wiley: New York, 1984.
(5) For a recent elegant study, see: Johnston, L. J.; Schepp, N. P. *J. Am. Chem. Soc.* **1993**, *115*, 6564.
(6) (a) Mariano, P. S. *Tetrahedron* **1983**, *39*, 3845. *Acc. Chem. Res.* **1983**, *16*, 130. (b) Mariano, P. S. *Organic Photochemistry*; Padwa, A., Ed.; Marcel Dekker: New York, 1987; Vol. 9, p 1.
(7) (a) Ohga, K.; Yoon, U. C.; Mariano, P. S. *J. Org. Chem.* **1984**, *49*, 213. (b) Lan, A. J. Y.; Heuckeroth, R. O.; Mariano, P. S. *J. Am. Chem. Soc.* **1987**, *109*, 2738. (c) Borg, R. M.; Heuckeroth, R. O.; Lan, A. J. Y.; Quillen, S. L.; Mariano, P. S. *J. Am. Chem. Soc.* **1987**, *109*, 2728. (d) Cho, I. S.; Tu, C. L.; Mariano, P. S. *J. Am. Chem. Soc.* **1990**, *112*, 3594.

0002-7863/94/1516-4211$04.50/0

investigations[8] probing the SET photochemistry of tertiary amine–enone systems, mechanistically intriguing and synthetically useful reactions driven by tertiary aminium radical α-CH deprotonation and α-desilylation (eq 1) were uncovered. The complimentary

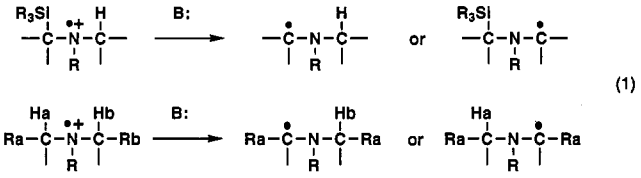

(1)

influences of solvent type and base strength on the relative rates (assessed by product analysis) of these competing α-heterolytic fragmentation processes were delineated[9] and then used as strategy elements in the design of chemoselective and regioselective photoaddition and photocyclization reactions.[10,11]

Even earlier, interest in tertiary aminium radical α-CH deprotonation reactions revolved about intense investigations[12,13] of amine–olefin, –arene, and –ketone SET-induced photoaddition reactions. Thorough product analyses of tertiary amine–stilbene photoaddition reactions by Lewis and his co-workers[13] first brought to light the effects of α-substituents on the relative rates of these α-CH deprotonation processes. Similarly, the selectivities observed in tertiary amine anodic oxidation reactions were also interpreted in terms of substituent effects on the rates of α-CH deprotonation of aminium radicals derived by one-electron oxidation.[14]

Continuing interest in this area of cation radical chemistry[15] has led to several recent efforts which have employed direct measurements to determine tertiary aminium radical α-CH deprotonation rates. Included here are the pulse radiolysis study of von Sonntag,[16] the stopped-flow investigation of Dinnocenzo,[17] and the derivative cyclic voltammetry determinations of Parker[18] (see below). Our attempts to understand how substituents and media govern the chemoselectivities (eq 1, $\sim H^+$ *vs* $\sim SiR_3^+$) and regioselectivities (eq 1, $\sim H_a^+$ *vs* $\sim H_b^+$) of tertiary aminium radical α-heterolytic fragmentation reactions guided us to the current investigation in which laser spectroscopic techniques were used to generate, characterize, and determine the decay rates of tertiary amine cation radicals. In this way, we have obtained α-CH deprotonation rates for cation radicals derived from para-substituted *N,N*-dimethylanilines **1–5** and α-substituted *N,N*-diphenyl-*N*-methylamines **7–13** and the rates of desilylation of the aminium radical from *N*-methyl-*N*-((trimethylsilyl)methyl)-aniline (**6**). These results along with observations of solvent, salt, and base strength effects are summarized and discussed below.

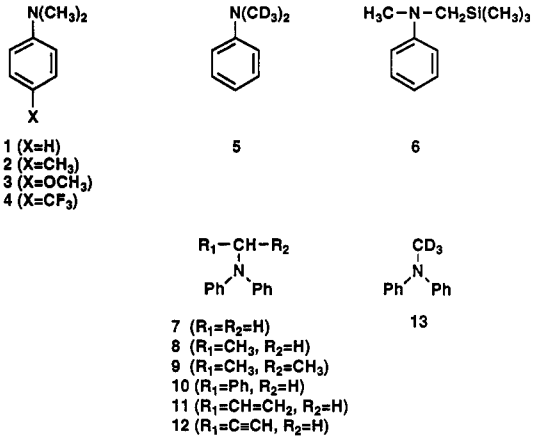

Results

Generation, Detection, and Decay Kinetics of the *N,N*-Dimethylaniline (DMA) Cation Radical. The first phase of our studies focused on the SET-photoinduced generation and detection of the DMA cation radical. As anticipated, laser excitation (308 nm, 6 ns, 50–60 mJ) of a deoxygenated solution of DMA (0.5 mM) and 1,4-dicyanobenzene (DCB) (50 mM) in 60:40 MeOH:MeCN (by volume) leads to generation of two transient absorption bands assigned as that for the DCB anion radical ($DCB^{\bullet-}$) (340 nm) and that for the DMA cation radical ($DMA^{\bullet+}$) (460 nm) (see eq 2 and Figure 1). These absorption maxima match those

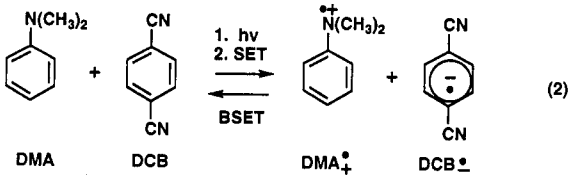

(2)

previously reported[19,20] for these species. Further, both bands decay with overall second-order kinetics (power dependence on the rate observed). Owing to the nature of our planned studies, it was important to determine the process responsible for decay of these ion radical intermediates. Analysis of the decay curves (Figures 2 and 3) in conjunction with the known[20] molar extinction coefficient of $DCB^{\bullet-}$ (3.4×10^4 $M^{-1}cm^{-1}$ at 340 nm) and the calculated[21] molar absorptivity of $DMA^{\bullet+}$ (6.5×10^3 $M^{-1}cm^{-1}$ at 460 nm) gives second-order rate constants of 1.29×10^{10} and 1.11×10^{10} M^{-1} s^{-1} for decay of the respective $DCB^{\bullet-}$ and $DMA^{\bullet+}$ species. The $DCB^{\bullet-}$ and $DMA^{\bullet+}$ decay rates are not dependent on α-CD substitution in the amine (*i.e.* from $PhN(CD_3)_2$). Thus, the equivalence of the decay rates and the lack of an isotope dependence suggest that the predominant mode of decay of these ion radicals is diffusion-controlled back electron transfer.

Having shown that $DMA^{\bullet+}$ can be generated and detected and that its decay kinetics can be accurately analyzed, we addressed the issue of medium effects on the ion radical lifetimes. Our purpose here was only to gain information about solvent and salt effects which would aid in our later (see below) interpretation of α-heterolytic fragmentation reactions of amine cation radicals. Accordingly, rate constants were determined for back electron transfer induced decay of $DMA^{\bullet+}$ and $DCB^{\bullet-}$ in media comprised of the solvents MeCN, EtOH, MeOH, and H_2O and in 60:40 MeOH:MeCN containing 0–0.1 M nBu_4NClO_4, $LiClO_4$, nBu_4NCl, nBu_4NBF_4, $nBu_4NO_3SCF_3$, and nBu_4NF. As the data in

(8) Yoon, U. C.; Mariano, P. S. *Acc. Chem. Res.* **1992**, *25*, 233.
(9) Hasegawa, E.; Xu, W.; Mariano, P. S.; Yoon, U. C.; Kim, J. U. *J. Am. Chem. Soc.* **1988**, *110*, 8099.
(10) Jeon, Y. T.; Lee, C. P.; Mariano, P. S. *J. Am. Chem. Soc.* **1991**, *113*, 8847.
(11) (a) Xu, W.; Mariano, P. S. *J. Am. Chem. Soc.* **1991**, *117*, 1431. (b) Xu, W.; Zhang, X. M.; Mariano, P. S. *J. Am. Chem. Soc.* **1991**, *113*, 8863.
(12) For a comprehensive review of amine SET photochemistry, see: (a) Pienta, N. J. *Photoinduced Electron Transfer*; Fox, M. A., Chanon, M., Eds.; Elsevier: New York, 1988; Part C. (b) Yoon, U. C.; Mariano, P. S.; Givens, R. S.; Atwater, B. W. *Advances in Electron Transfer Chemistry*; Mariano, P. S., Ed.; JAI-Press: Greenwich, CT, 1994, in press.
(13) (a) Lewis, F. D. *Acc. Chem. Res.* **1986**, *19*, 401. (b) Lewis, F. D.; Ho, T. I.; Simpson, J. T. *J. Am. Chem. Soc.* **1982**, *104*, 1924. (c) Lewis, F. D.; Ho, T. I.; Simpson, J. T. *J. Org. Chem.* **1981**, *46*, 1077.
(14) See ref 4 and also Smith P. J.; Mann, C. K. *J. Org. Chem.* **1969**, *34*, 1821. Lindsay-Smith, J. R.; Mead, L. A. V. *J. Chem. Soc., Perkin Trans. 2* **1973**, 206. Lindsay-Smith, J. R.; Masheder, D. *J. Chem. Soc., Perkin Trans 2* **1976**, 47.
(15) (a) Nelsen, S. F.; Ippoliti, J. T. *J. Am. Chem. Soc.* **1986**, *108*, 4879. (b) Chow, Y. L.; Danen, W. C.; Nelsen, S. F.; Rosenblatt, D. *Chem. Rev.* **1978**, *78*, 243.
(16) Das, S.; von Sonntag, C. *Z. Naturforsch.* **1986**, *416*, 505.
(17) Dinnocenzo, J. P.; Banach, T. E. *J. Am. Chem. Soc.* **1989**, *111*, 8646.
(18) Parker, V. D.; Tilset, M. *J. Am. Chem. Soc.* **1991**, *113*, 8778.
(19) Jones, G.; Malba, V. *Chem. Phys. Lett.* **1985**, *119*, 105.
(20) Robinson, E. A.; Schulte-Frohlinde, D. *J. Chem. Soc., Faraday Trans. 1*, **1973**, *69*, 707.
(21) The molar absorptivity of $DMA^{\bullet+}$ at 460 nm was determined by using the ratio of the absorbance at 340 nm for $DCB^{\bullet-}$ to that at 460 nm and the known extinction coefficient of 6.5×10^3 M^{-1} cm^{-1} for $DCB^{\bullet-}$ assuming a 1:1 ratio of these ion radicals are formed.

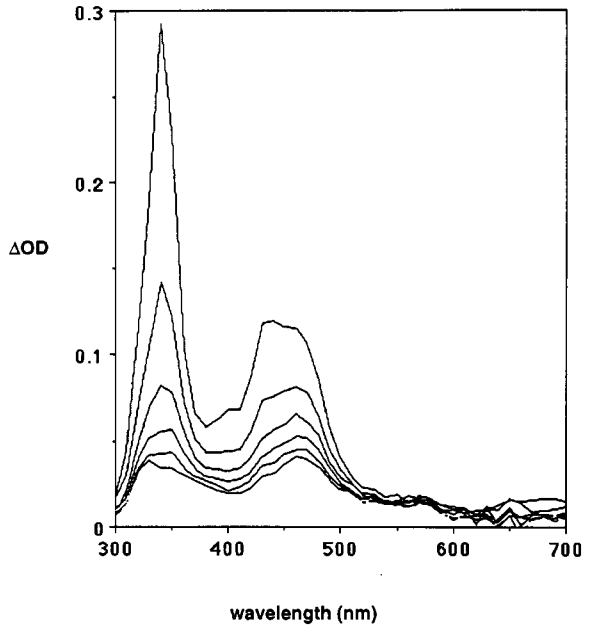

Figure 1. Transient absorption spectra following 308-nm excitation of 0.5 mM DMA and 50 mM DCB in 60:40 (volume) MeOH:MeCN at 2, 4, 6, 8, 10, 12, and 14 μs.

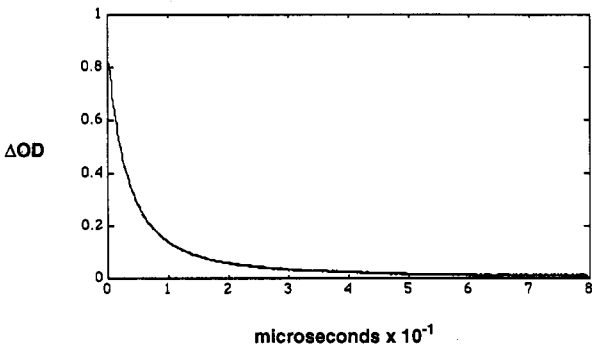

Figure 2. Decay of $DCB^{\bullet-}$ at 340 nm after excitation of a solution of 0.5 mM DMA and 50 mM DCB in 60:40 CH_3OH:CH_3CN. Points are experimental data, and the solid curve represents kinetics calculated upon the basis of second-order decay.

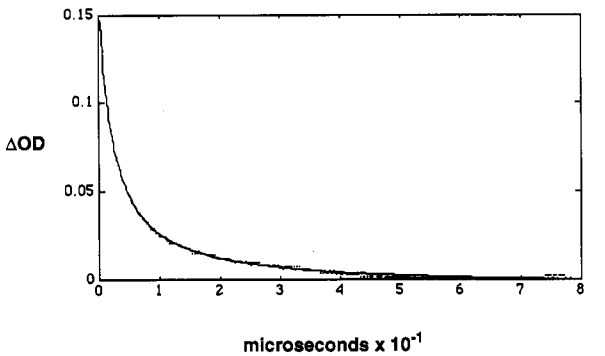

Figure 3. Decay of $DMA^{\bullet+}$ at 460 nm after excitation of a solution of 0.5 mM DMA and 50 mM DCB in 60:40 CH_3OH:CH_3CN. Points are experimental data, and the solid curve represents kinetics calculated upon the basis of second-order decay.

Figures 4 and 5 and summarized in Table 1 show, the rate constants ($k\epsilon^{-1}$) for $DMA^{\bullet+}$ decay decrease by nearly 1 order of magnitude with increasing concentrations of the salts listed above. The magnitude of this effect associated with $LiClO_4$ and nBu_4NClO_4 is equal and larger than that for the other tetra-*n*-butylammonium salts. Also, the attenuating effects of the salts

(22) Murov, S. L. *Handbook of Photochemistry*; Marcel Dekker: New York, 1973; p 55.

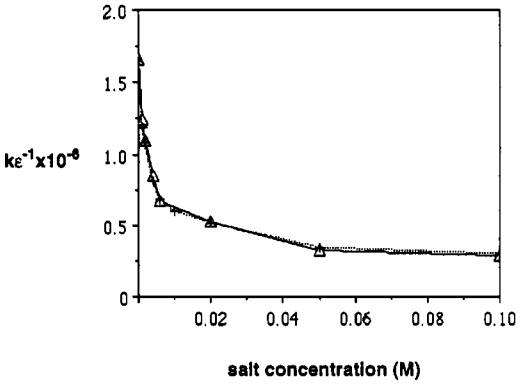

Figure 4. Rate ($k\epsilon^{-1}$) of $DMA^{\bullet+}$ decay at 460 nm *vs* salt concentrations following excitation of solutions of DMA and DCB in 60:40 MeOH:MeCN containing nBu_4NClO_4 (solid line) and $LiClO_4$ (dotted line).

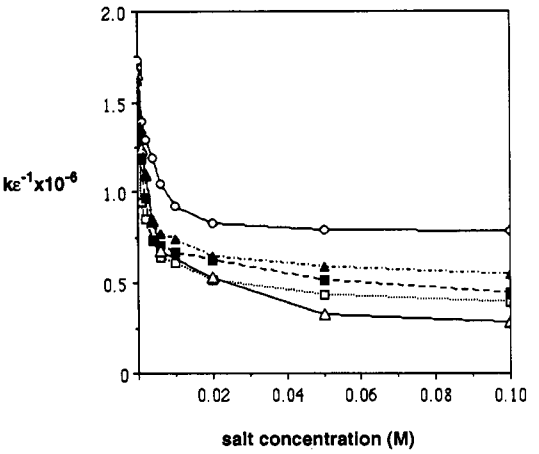

Figure 5. Rate ($k\epsilon^{-1}$) of $DMA^{\bullet+}$ decay at 460 nm *vs* salt concentrations following excitation of solutions of DMA and DCB in 60:40 MeOH:MeCN containing nBu_4N–ClO_4 (empty triangles), –Cl (empty squares), $-BF_4$ (filled squares), $-O_3SCF_3$ (filled triangles), and –F (empty circles).

Table 1. Solvent and Salt Effects on the Second-Order Rate Constants (25 °C) for Decay of the Dimethylaniline Cation Radical

solvent	salt (0.1 M)	$k \times 10^{-10}$ (M^{-1} s^{-1})	$\eta \times 10^{-2}$ (P)[a]	$k_{diff} \times 10^{10}$ (M^{-1} s^{-1})[b]
EtOH		0.70	1.08	0.61
MeOH		1.05	0.55	1.21
MeCN		2.05	0.35	1.91
60:40 MeOH:MeCN		1.11		
60:40 MeOH:MeCN	$LiClO_4$	0.17		
60:40 MeOH:MeCN	nBu_4NClO_4	0.17		
60:40 MeOH:MeCN	nBu_4NCl	0.25		
60:40 MeOH:MeCN	nBu_4NBF_3	0.28		
60:40 MeOH:MeCN	$nBu_4NO_3SCF_3$	0.34		
60:40 MeOH:MeCN	nBu_4NF	0.49		

[a] Viscosity in Poise (g/(s·cm)) at 25 °C (ref 22). [b] Calculated by use of $k_{diff} = 8RT/3000\eta$ at 25 °C.

are the same for decay of both the $DMA^{\bullet+}$ and $DCB^{\bullet-}$ transients. Finally, the salt effects display a saturation behavior; that is, the ion radical decay rates reach minimum values above salt concentrations of *ca.* 0.05–0.1 M.

The absorption spectral profiles for the $DMA^{\bullet+}$ and $DCB^{\bullet-}$ transients generated by laser excitation of MeCN, EtOH, MeOH, and H_2O solutions of DMA and DCB are identical to those for these radical ions in 60:40 MeOH:MeCN. Also, both of these species have equivalent decay rates in these solvents. However, as demonstrated by the data accumulated in Figure 6 and Table 1, the nature of the solvent has a definite effect on the second-order rate constants for simultaneous decay of $DMA^{\bullet+}$ and $DCB^{\bullet-}$. The decrease in the $DMA^{\bullet+}$ decay rate in proceeding from MeCN (2.1×10^{10} M^{-1} s^{-1}), to MeOH (1.1×10^{10} M^{-1} s^{-1}) to EtOH (7×10^9 M^{-1} s^{-1}) appears to be best correlated with the bimolecular

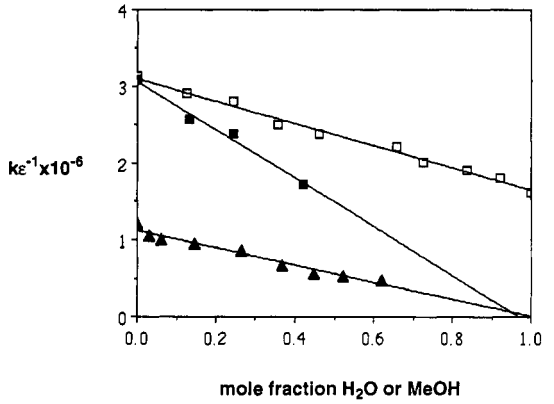

Figure 6. Rate ($k\epsilon^{-1}$) of DMA$^{\bullet+}$ decay at 460 nm *vs* mole fractions of MeOH in MeCN (empty squares), H_2O in MeCN (filled squares), and H_2O in EtOH (filled triangles) following excitation of solutions of DMA and DCB.

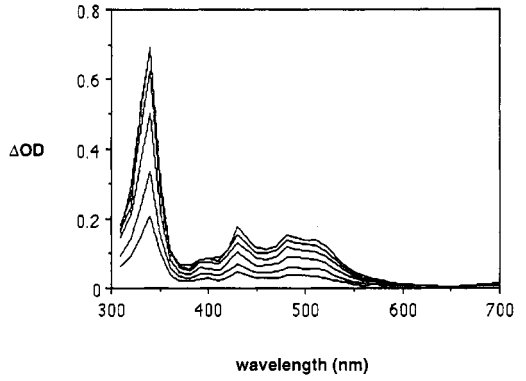

Figure 7. Transient absorption spectra following 308-nm excitation of 0.5 mM TMS-substituted aniline **6** and 50 mM DCB in MeCN at 0.2, 0.5, 1, 2, 4, 7, and 10 μs.

diffusion rates in these solvents, which are governed by their viscosity (Table 1).

Decay Kinetics for the *N*-Methyl-*N*-((trimethylsilyl)methyl)-aniline Cation Radical. The SET-photochemical methodology described above was used to generate the *N*-methyl-*N*-((trimethylsilyl)methyl)aniline (**6**) cation radical (TMSA$^{\bullet+}$) (eq 3)

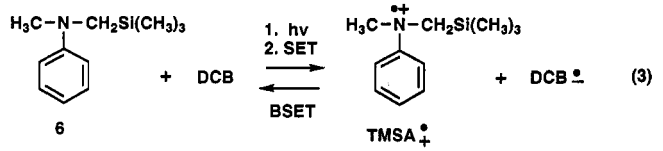

(3)

and to analyze its decay kinetics. The spectrum produced by irradiation (308 nm) of a deoxygenated MeCN solution of **6** (0.5 mM) and DCB (13 mM) is comprised of bands for TMSA$^{\bullet+}$ (480 nm, $\epsilon = 7.4 \times 10^3$ M^{-1} s^{-1}) and DCB$^{\bullet-}$ (340 nm) (Figure 7). Analysis of the decay profiles (Figures 8 and 9) gives the second-order rate constants 1.2×10^{10} and 9.9×10^9 M^{-1} s^{-1} (25 °C) for decay of the respective transients.

The rate of decay of TMSA$^{\bullet+}$ (and not of DCB$^{\bullet-}$, see Figure 10) is greatly accelerated by the presence of silophilic substances such as MeOH, H_2O, and nBu_4NF. Disappearance of the TMSA$^{\bullet+}$ absorption at 480 nm displays a pseudo-first-order kinetic dependence on these substances in MeCN solutions. A plot (Figure 11) of the TMSA$^{\bullet+}$ decay rate *vs* MeOH concentration (*ca.* 2–25 M) in MeCN is linear with a positive slope. The data yield a second-order rate constant of 8.9×10^5 M^{-1} s^{-1} for MeOH-induced decay of TMSA$^{\bullet+}$. In contrast, a two-component dependence (Figure 12) of TMSA$^{\bullet+}$ decay on water concentration (*ca.* 1–20 M) in MeCN is observed. By using data in the near linear ([H_2O] = 0–5 M) region of this plot, it is possible to calculate

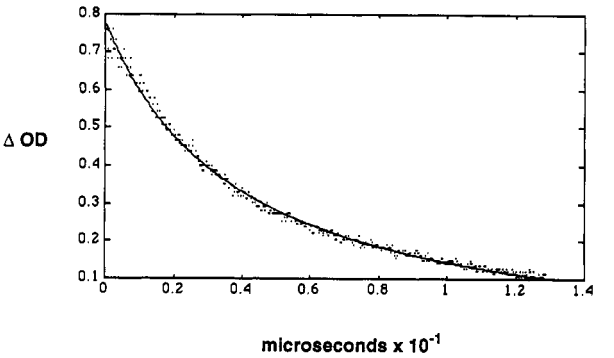

Figure 8. Decay of DCB$^{\bullet-}$ at 340 nm after excitation of a solution of 0.5 mM **6** and 50 mM DCB in MeCN. Points are experimental data, and the solid curve represents kinetics calculated upon the basis of second-order decay.

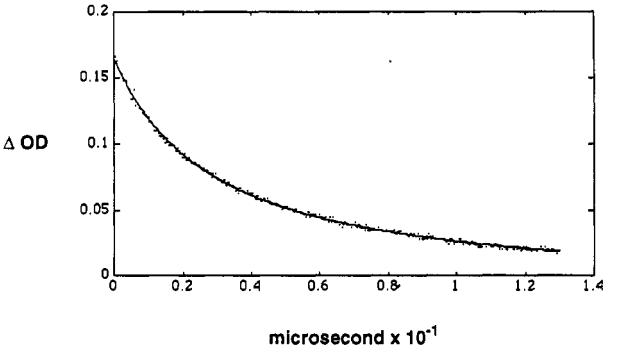

Figure 9. Decay of TMSA$^{\bullet+}$ at 480 nm after excitation of a solution of 0.5 mM **6** and 50 mM DCB in MeCN. Points are experimental data, and the solid curve represents kinetics calculated upon the basis of second-order decay.

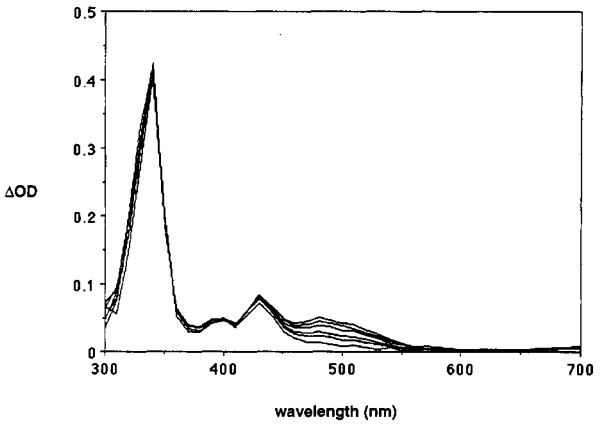

Figure 10. Transient absorption spectra following 308-nm excitation of 0.5 mM **6**, 13 mM DCB, and 5 M H_2O in MeCN at 0.2, 0.5, 1, 1.5, 2, and 5 μs.

a second-order rate constant of 1.3×10^6 M^{-1} s^{-1} for the H_2O + TMSA$^{\bullet+}$ decay process. Finally, a more dramatic effect is seen with the potent silophile nBu_4NF. The decay rate *vs* [nBu_4NF] (*ca* 0–1 mM) data plotted in Figure 13 yield a rate constant of 3.2×10^9 M^{-1} s^{-1} for fluoride-promoted TMSA$^{\bullet+}$ decay.

α-CH Deprotonation Rates for Dimethylaniline Cation Radicals. A number of preliminary experiments were performed to demonstrate that this methodology can be reliably employed in the determination of tertiary aminium radical α-CH deprotonation rates. The effects of base (nBu_4NOAc) on the decay of the DMA$^{\bullet+}$ and DCB$^{\bullet-}$ transients were evaluated. As seen by viewing the spectra in Figure 14 and plots in Figure 15, the presence of nBu_4NOAc in 60:40 MeOH:MeCN results in an increase in the rate of DMA$^{\bullet+}$ decay and not in that of DCB$^{\bullet-}$. Also, the effects of nBu_4NOAc and the weaker base $nBu_4NO_2CCF_3$ on the rate of DMA$^{\bullet+}$ decay are linear (Figure 15). Plots of rate *vs* base

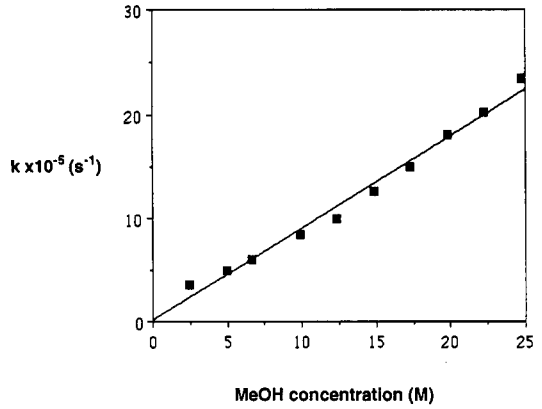

Figure 11. Rate of TMSA$^{\bullet+}$ decay at 480 nm *vs* concentration of MeOH in MeCN.

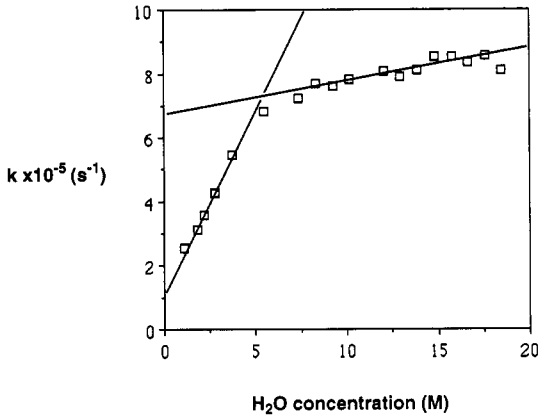

Figure 12. Rate of TMSA$^{\bullet+}$ decay at 480 nm *vs* concentration of H_2O in MeCN.

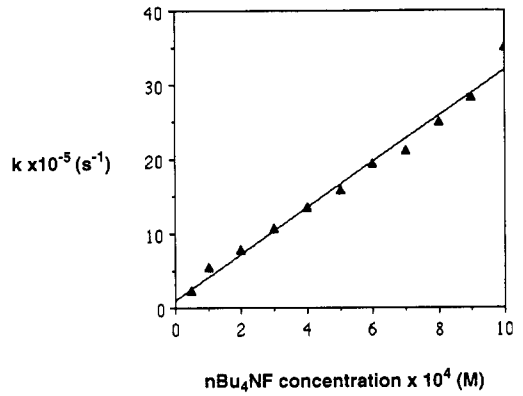

Figure 13. Rate of TMSA$^{\bullet+}$ decay at 480 nm *vs* concentration of nBu_4NF in MeCN.

concentration give second-order rate constants of 3.1×10^5 and 8.0×10^4 M^{-1} s^{-1} for the respective bases. In order to avoid problems associated with salt effects on the DMA$^{\bullet+}$ lifetime, the solutions used for these measurements containing base concentrations in the range 0–0.6 M were maintained at a constant salt concentration of 0.6 M by the addition of corresponding amounts of nBu_4NClO_4. Finally, similar measurements made on the cation radical derived from the aniline-d_6 **5** give a k_H/k_D value of 3.6 (25 °C, 60:40 MeOH:MeCN, nBu_4NOAc as the base). The combined results (Table 2) show that the carboxylate-promoted decay of DMA$^{\bullet+}$ is associated with an α-CH bond cleavage process involving proton transfer to the base.

To probe the effects of para-substituents on DMA$^{\bullet+}$ α-CH kinetic acidity, the rates of nBu_4NOAc-dependent decay of cation radicals, derived from the dimethylanilines **2–4** with *p*-CH_3, *p*-OCH_3, and *p*-CF_3 groups, were determined. Rate constants

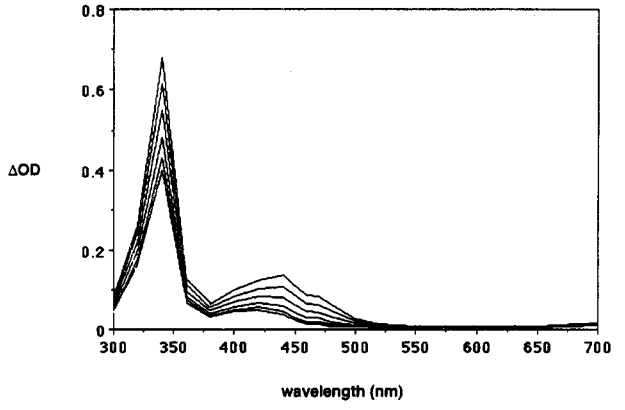

Figure 14. Transient absorption spectra following 308-nm excitation of 0.5 mM DMA and 50 mM DCB in 60:40 MeOH:MeCN containing 0.6 M nBu_4NOAc at 1, 2, 3, 5, 7, 10, and 15 μs.

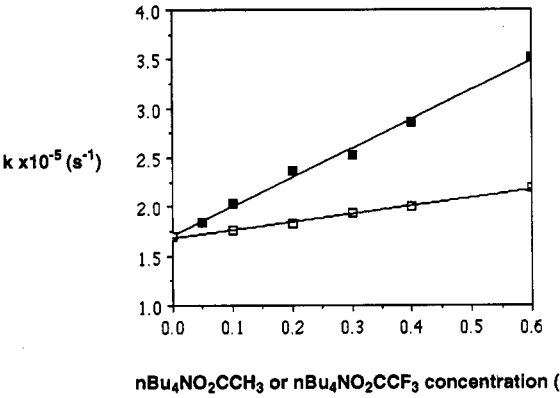

Figure 15. Rate of DMA$^{\bullet+}$ decay at 460 nm *vs* concentrations of nBu_4NOAc (filled squares) and $nBu_4NO_2CCF_3$ (empty squares) in 60:40 MeOH:MeCN.

Table 2. Rate Constants for Base-Promoted Decay of the Dimethylaniline Cation Radical in 60:40 MeOH:MeCN

aniline precursor	base	k (M^{-1} s^{-1}) at 25 °C
$PhN(CH_3)_2$	nBu_4NOAc	3.1×10^5
$PhN(CD_3)_2$	nBu_4NOAc	8.6×10^4
$PhN(CH_3)_2$	$nBu_4NO_2CCF_3$	8.0×10^4

Table 3. Rate Constants for nBu_4NOAc-Promoted Decay of Para-Substituted Dimethylaniline Cation Radicals in 60:40 MeOH:MeCN

para-substituent	k (M^{-1} s^{-1}) at 25 °C	E_{ox}[a] (V *vs* SCE)	λ_{max} (nm)
OMe	2.0×10^4	+0.49	480
CH_3	1.1×10^5	+0.65	460
H	3.1×10^5	+0.71, +0.65	460
CF_3	2.5×10^6		440

[a] Taken from ref 23.

resulting from decay rate *vs* [nBu_4NOAc] data for 60:40 MeOH:MeCN solutions at 25 °C and constant (0.6 M) salt concentration are given in Table 3 along with the known oxidation potentials of the precursor anilines and the absorption maxima of the corresponding cation radicals.

α-Substituent Effects on Tertiary Amine Cation Radicalα-CH Kinetic Acidity. The *N*-substituted-*N*,*N*-diphenylamines **7–13** were used to assess the effects of α-substituents on the rates of α-CH deprotonation of amine cation radicals. While these amines are properly structured for the designed purpose, their documented[24] propensity to undergo excited-state electrocyclization to produce azomethine ylids (eq 4) was an initial concern. Indeed,

(23) Seo, E. T.; Nelson, R. F.; Frtisch, J. M.; Marcoux, L. S.; Leddy, O. W.; Adams, R. N. *J. Am. Chem. Soc.* **1966**, *88*, 3498.
(24) Forster, E. W.; Grellman, K. H. *J. Am. Chem. Soc.* **1973**, *95*, 3108.

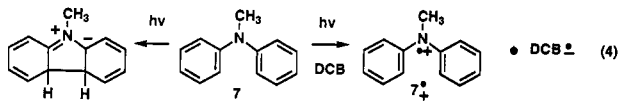

excitation (308 nm) of Ph_2NMe (7) in 25:75 MeOH:MeCN does lead to formation of a 610-nm absorbing transient (Figure 16), identified previously[24] as the ylide shown in eq 4. This transient undergoes slow, [nBu_4NOAc]-independent decay. In contrast, irradiation of a mixture of 0.1 M DCB and 7 (0.5 mM) leads instead to simultaneous production of $DCB^{\bullet-}$ and a new transient absorbing at 645 nm (7.8×10^3 $M^{-1}cm^{-1}$) (Figure 17). The 645-nm species is assigned as the cation radical of 7 (*i.e.*, $7^{\bullet+}$). As expected, $DCB^{\bullet-}$ and $7^{\bullet+}$ decay at equivalent (1.2×10^{10} M^{-1} s^{-1}, 25 °C) diffusion-controlled rates (Figures 18 and 19). Moreover, the rate of $7^{\bullet+}$ decay is a linear function of [nBu_4-NOAc] with a derived second-order rate constant of 9.5×10^5 M^{-1} s^{-1} (25 °C, 25:75 MeOH:MeCN) and a k_H/k_D value (comparing $7^{\bullet+}$ and $13^{\bullet+}$ decay) of 2.81. Finally, cation radicals from the variously α-substituted diphenylamines **8–12** were generated by this SET-photochemical method and their decay kinetics were measured. The rate constants for nBu_4NOAc-induced decay of these transients (given along with their absorption maxima in Table 4) show a pronounced dependence on the nature and degree of α-substitution.

Discussion

Pathways for Amine Cation Radical Generation and Decay. The overall mechanistic sequence for amine cation generation used in these laser spectroscopic studies involves photoinduced electron transfer from the aniline derivatives to the singlet excited state[26] of DCB. The prediction that these processes should be thermodynamically ($\Delta G_{SET} < 0$) and, consequently, kinetically ($k_{SET} = ca.\ k_{diff}$)[27] favorable is based on a consideration of the redox potentials of the amine donors (*e.g.* $E_{1/2}(+) = ca.$ +0.7 V for DMA)[4a] and DCB^{S1} ($E_{1/2}(-) = ca.$ +2.6 V).[28] It is likely that SET in these donor–acceptor pairs results in direct formation of either solvent-separated (SSIRP) or contact (CIRP) ion radical pairs,[25] both with singlet multiplicity. Prior to the onset of transient detection in the laser experiments (*ca.* 10 ns), competitive reactions of the ion radical pairs can occur to produce neutral ground-state reactants (back electron transfer in SSIRP and/or CIRP) or fully solvated free ion radicals. The latter pathway is favorable in highly polar media like the MeCN–MeOH solvent systems employed in these experiments. Thus, it is reasonable to expect that the ion radicals whose kinetics are scrutinized in these laser spectroscopic studies are free species.

Several observations support both this proposal and the conclusion that the major pathway for decay of the free ion radicals in the absence of added bases or nucleophiles involves diffusion-controlled back electron transfer. Specifically, the second-order nature and equal rate constants for decay of each of the amine cation radicals and the DCB anion radical are consistent with involvement of free, charged radical intermediates. Furthermore, the strict dependence of these rates on solvent viscosity is another indicator of diffusion-controlled decay of free transients. Finally, the ion radical decay rates in the absence of added base show no d-isotope dependence, a result not expected if decay were by

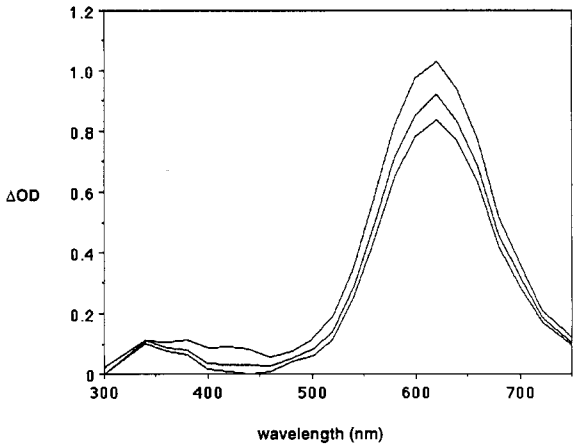

Figure 16. Transient absorption spectra following 308-nm excitation of 0.5 mM 7 in 25:75 MeOH:MeCN at 10, 100, and 400 μs.

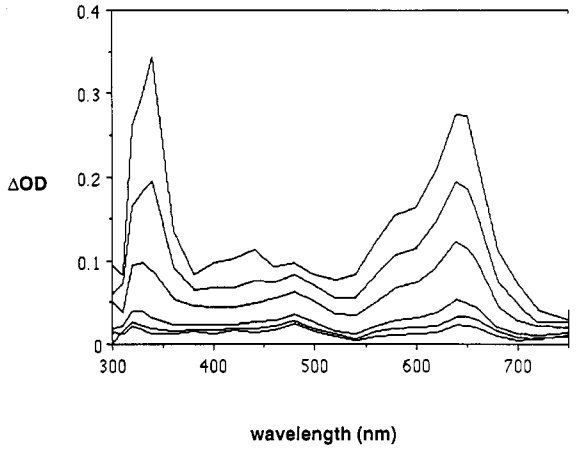

Figure 17. Transient absorption spectra following 308-nm excitation of 0.5 mM 7 and 0.1 M DCB in 25:75 MeOH:MeCN at 1, 2, 4, 10, 15, and 20 μs.

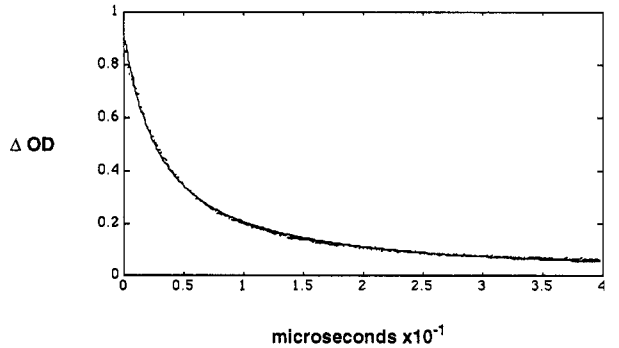

Figure 18. Decay of $DCB^{\bullet-}$ at 340 nm after excitation of a solution of 0.5 mM 7 and 0.1 M DCB in 25:75 CH_3OH:CH_3CN. Points are experimental data, and the solid curve represents kinetics calculated upon the basis of second-order decay.

proton transfer[29] from the amine cation to the cyanoarene anion radical (eq 5).

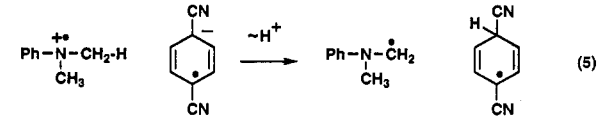

As part of experimentation to define conditions under which amine cation radical α-CH deprotonation rates could be accurately measured, the effects of nonbasic salts on the rates of $DMA^{\bullet+}$

(25) (a) The absorption maximum for this cation radical in MeCN, derived by irradiation of benzophenone *N*-methyl-*N*,*N*-diphenylamine mixtures, has been reported to be 635 nm (ref 25b). (b) Manring, L. E.; Peters, K. S. *J. Am. Chem. Soc.* **1985**, *107*, 6452.

(26) (a) ISC from DCB^{S1} is known to be slow (ref 26b). (b) Borg, R. M.; Arnold, D. R.; Cameron, T. S. *Can. J. Chem.* **1984**, *62*, 1785.

(27) Rehm, D.; Weller, A. *Isr. J. Chem.* **1970**, *8*, 259.

(28) (a) Calculated on the basis of $E_{1/2}(-) = ca.$ −1.6 V and $E_{0,0}^{S1} = ca.$ 98 kcal/mol (ref 28b,c) for DCB. (b) Wayner, D. D. M. *Handbook of Organic Photochemistry*; Scaiano, J. C., Ed.; CRC Press: Boca Raton, FL, 1987; Vol. 2, p 395. (c) Arnold, D. R.; Snow, M. S. *Can. J. Chem.* **1985**, *66*, 3012.

(29) Proton transfer from tertiary amine cation radicals with pK_a's of *ca.* 8–10 for $DCB^{\bullet-}$ ($pK_a < 0.1$, ref 20) should be slow.

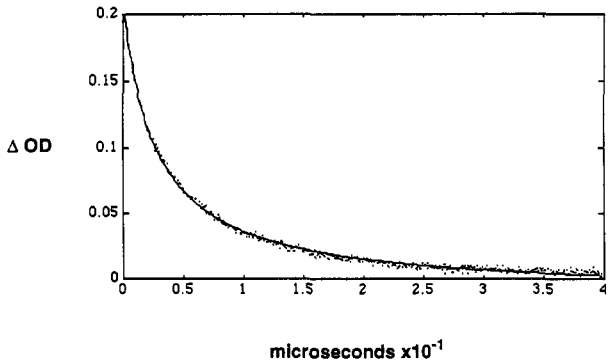

Figure 19. Decay of $7^{\bullet+}$ at 645 nm after excitation of a solution of 0.5 mM 7 and 0.1 M DCB in 25:75 CH_3OH:CH_3CN. Points are experimental data, and the solid curve represents kinetics calculated upon the basis of second-order decay.

Table 4. Rate Constants for nBu_4NOAc-Promoted Decay of α-Substituted *N,N*-Diphenyl-*N*-methylamine Cation Radicals in 25:75 MeOH:MeCN

α-substituents in $Ph_2NCHR_1R_2$			
R_1	R_2	k (M^{-1} s^{-1}) at 25 °C	λ_{max} (nm)
H	H	9.5×10^5	645
CH_3	H	2.3×10^5	650
CH_3	CH_3	1.7×10^5	660
Ph	H	3.2×10^6	680
$CH{=}CH_2$	H	2.6×10^6	670
$C{\equiv}CH$	H	7.0×10^7	675

and $DCB^{\bullet-}$ decay by BSET were probed. As the data displayed in Figures 4 and 5 demonstrate, the lifetimes of the ion radical transients increase upon the addition of increasing concentrations of tetra-*n*-butylammonium salts. In general, the effects observed are (1) small (for [salt] = 1–0.06 M, the decay rates decrease *ca.* 5-fold), (2) dependent on the nature of the counter anion (ClO_4^- > Cl^-, BF_4^-, $CF_3SO_3^-$ > F^-), and (3) saturating at salt concentrations exceeding *ca.* 0.06 M. It should be noted that a related effect by $Mg(ClO_4)_2$ on BSET-promoted decay between 1,4-dicyanonaphthalene anion radical ($DCN^{\bullet-}$) and *trans*-stilbene cation radicals has been noted earlier by Goodson and Schuster[30] and interpreted in terms of Mg^{2+} complexation of $DCN^{\bullet-}$. Our results show that anions can have a similar stabilizing influence on amine cation radicals. Moreover, the results suggest that attention must be paid to total salt concentration in designing experiments to accurately assess the effects of basic salts on amine cation radical decay.

Tertiary Amine Cation Radical α-CH Kinetic Acidities. Perhaps the most significant observations made in the current study are those which relate to the α-CH kinetic acidities of tertiary amine cation radicals. As mentioned briefly in the Introduction, this issue has been of central interest to a number of earlier efforts probing SET-photochemical and anodic oxidation reactions of amines. In order to place our results in proper context, an overview of the early observations will be given first followed then by an interpretation and discussion of the data we have accumulated.

Perhaps the first detailed discussion of trialkylamine cation radical α-CH acidity is found in Nelsen and Ippoliti's[15a] 1986 paper in which the Nicholas–Arnold method[31] was used to estimate thermodynamic acidities of these species. On the basis of the large pK_a value of *ca.* 15 (in MeCN) these workers calculated for an *N*-adamantyl-9-azaadamantane cation radical, they suggested that α-CH deprotonation of tertiary aminium radicals by the corresponding neutral amines should be slow relative to a possibly more facile H-atom-transfer (*i.e.* Hoffman–Loefler–Freytag like) route for α-amino radical production (eq 6).

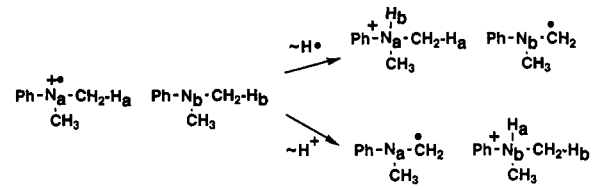

The pulse radiolysis experiments of Das and von Sonntag[16] represent an early approach to gaining information about tertiary amine cation radical kinetic α-CH acidity. Steady-state radiolysis conditions were used to generate mixtures of the trimethylamine cation radical, its α-amino radical counterpart, and its N-protonated α-amino radical analog. Analysis of the equilibrium product ratios and the time-dependent changes in approaching equilibrium provided a value of 8 for the pK_a of the tertiary cation radical and a rate constant of 7.3×10^8 M^{-1} s^{-1} for proton transfer to trimethylamine (eq 7). Although interpreted in this way, these results are also consistent with an H-atom-transfer pathway for α-amino radical and ammonium cation production.

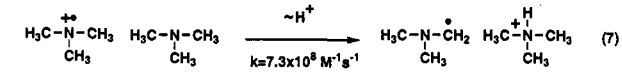

More recently, Dinnocenzo and Banach[17] described an interesting technique for directly assessing the kinetics of α-CH proton removal from stable tertiary aminium radicals. Deprotonation reactions of the stable salt $(p\text{-}CH_3OC_6H_4)_2NCH_3^{\bullet+}AsF_6^-$ (pK_a (MeCN) = *ca.* 10) by quinuclidine bases were analyzed by stopped-flow methods. While limited to studies with stable cation radicals,[32] these experiments provided detailed information about the α-CH deprotonation reactions including $k_{(CH3)}/k_{(CD3)} = 7.7$ (15 °C), $\Delta H^{\ddagger} = 3.7$ kcal/mol, $\Delta S^{\ddagger} = -22.3$ ea, and Bronstead $\beta = 0.63$.

The most recent investigation in which tertiary amine cation radical α-CH kinetic acidity was probed used a derivative cyclic voltammetry methodology.[18] Parker and Tilset employed this technique to measure the rates of both acetate ion- and pyridine-induced α-CH deprotonation reactions of para-substituted *N,N*-dimethylaniline cation radicals in MeCN. The most pertinent finding of this study is that a relationship exists between the thermodynamic and kinetic acidities of these cation radicals. Specifically, the rate constants for acetate-induced α-CH deprotonation of the anilinium radicals are inversely related to the estimated pK_a values which vary with para-substituents in the manner expected.[31] Para-electron-withdrawing groups, for example, lower the pK_a values and enhance the rate constants for α-CH deprotonation *via* their influence on amine oxidation potentials (see below) and, as a result, on cation radical stability. Several less clear aspects of the Parker–Tilset results include the abnormally high d-isotope effects (*ca.* 5–22) associated with the pyridine-induced α-CH deprotonation processes and the large differences in the enthalpies (20 *vs* 2–13 kcal/mol) and entropies (35–53 *vs* −15 to −29 eu) of activation for the respective acetate ion- and pyridine-promoted α-CH deprotonations.

In contrast to the methods employed previously for kinetic analysis of tertiary aminium radical α-CH deprotonation reactions, the laser spectroscopic technique has many obvious advantages. First, the ion radical species are generated under isotropic conditions. Thus, no questions exists about the degree of their association with other charged radicals or electrode surfaces. In addition, a large variety of aminium radicals can be probed in this way without limitations associated with their

(30) Goodson, B.; Schuster, G. B. *Tetrahedron Lett.* **1986**, *27*, 3123. See also: Loupy, A.; Tchoubar, B.; Astruc, D. *Chem. Rev.* **1992**, *92*, 1141.
(31) Nicholas, A. M. P.; Arnold, D. R. *Can. J. Chem.* **1982**, *60*, 2166. Nicholas, A. M. P.; Boyd, R. J.; Arnold, D. R. *Can. J. Chem.* **1982**, *60*, 3011.
(32) Application of the Dinnocenzo–Banach method (ref 17) appears limited to stable cation radicals with deprotonation rates that are less than *ca.* 10^3 M^{-1} s^{-1}.

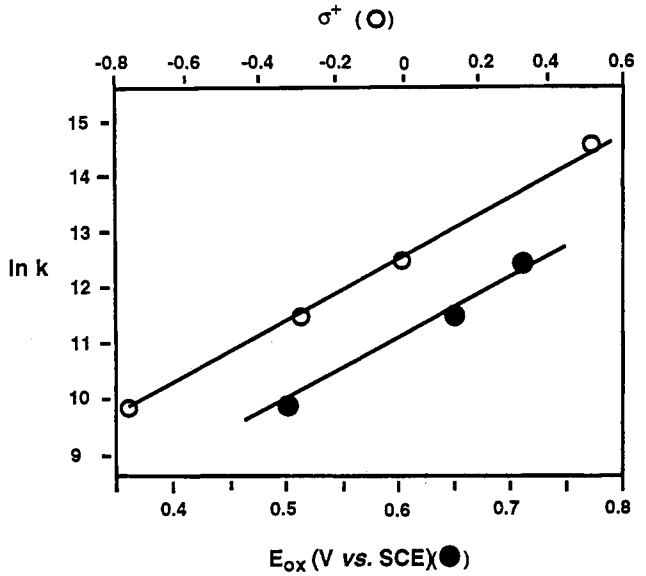

Figure 20. Plots of ln k (MeCN, 25 °C) for acetate-promoted deprotonation of para-substituted *N,N*-dimethylanilinium radicals *vs* the corresponding aniline oxidation potentials ($E°$) (filled circles) and the σ^+ constants of the respective para-substituents (empty circles).

synthesis and stability. Finally, when low concentrations of precursor amines and high concentrations of added bases are used, it is possible to rule out the H-atom abstraction pathway as being responsible for ion radical decay. Indeed, the dependencies of $DMA^{\bullet+}$ decay on base strength and concentration in conjunction with the reasonable primary d-isotope effects all point to α-CH deprotonation as the kinetically significant process involved in tertiary aminium radical decay in the presence of carboxylate anion bases.

One of the main goals of this effort was to delineate how substituents govern the kinetic α-CH acidities of tertiary amine cation radicals. If these reactive intermediates behave as "normal" acids, one might anticipate that kinetic acidity would parallel thermodynamic acidity and, consequently, that kinetic acidity would be influenced by substituents in a predictable fashion. Indeed, as Nicholas and Arnold[31] have clearly summarized, the pK_a values of cation radicals are related to the oxidation potential ($E°$) of the neutral precursor and the bond dissociation energy (BDE) of the C–H bond undergoing cleavage (eq 8).

$$pK_a = \frac{-E°}{0.059} + \frac{BDE - 37.5}{1.36} \qquad (8)$$

In accord with these considerations, para-ring substituents in dimethylanilinium radicals should alter pK_a values by their influence on $E°$, *i.e.* the pK_a should decrease as the electron-donating ability of the substituent decreases. This can be viewed as a substituent effect on the stability of the cation radical. Indeed, the rate constants for acetate-promoted deprotonation of the anilinium radicals respond to para-substitution in the same fashion as do the pK_a values. The linear correlations seen between ln k and both the aniline oxidation potentials and σ^+ constants of the para-substituents (Figure 20) demonstrate clearly that a close relationship exists between kinetic and thermodynamic acidities of the tertiary amine cation radicals.[33]

Likewise, α-substitution should govern the α-CH pK_a values of tertiary amine cation radicals principally through a control of α-CH bond dissociation energies. Thus, substituents which stabilize the resulting α-amino radical (*i.e.* lower BDE) should

(33) (a) This same parallel exists for toluene and related ring methyl substituted cation radicals (ref 33b). (b) Schlesener, C. J.; Amatore, C.; Kochi, J. K. *J. Am. Chem. Soc.* **1984**, *106*, 3567, 7472. Masnovi, J. M.; Sankararaman, S.; Kochi, J. K. *J. Am. Chem. Soc.* **1989**, *111*, 2263. Sehested, K.; Holcman, J. *J. Phys. Chem.* **1978**, *82*, 651.

Table 5. Relative Rates of α-CH Deprotonation of α-Substituted Tertiary Amine Cation Radicals from Product Distribution and Laser Spectroscopy Studies

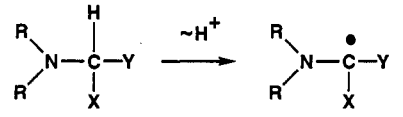

			relative rates		
entry	X	Y	per-H from stilbene–amine SET photo-additions[a]	per-H from amine–enone SET photo-cyclizations[b]	from rate constants for *N*-alkyl-*N,N*-diphenyl-aminium radical decay[c]
a	H	H	1.1	0.1	0.3
b	H	CH_3	0.5	0.2	0.1
c	CH_3	CH_3	<0.05		0.05
d	H	Ph	1	1	1
e	H	$CH{=}CH_2$	0.5	1.9	0.8
f	H	C≡CH	111	3.9	22

[a] Taken from ref 13. [b] Taken from ref 11. [c] This work, Table 4.

enhance the thermodynamic acidities of these charged radical intermediates. Bordwell and his co-workers[34] have presented a number of examples showing that radical-stabilizing C-9 and benzylic substituents lower the pK_a's of the respective fluorene[34a] and toluene[34b] cation radicals. Stabilization of the transition state for α-CH deprotonation by radical-stabilizing groups should also lead to enhanced kinetic acidity. As pointed out earlier by Lewis and his co-workers,[13] steric and/or stereoelectronic effects associated with α-substitution could also be important in governing the rates of tertiary amine cation radical α-CH deprotonation. Product distributions from SET-induced stilbene–tertiary amine photoaddition reactions suggest that alkyl substitution slows the rates of α-CH proton transfer from the tertiary aminium radicals to the stilbene anion radicals in contact ion radical pairs (see Table 5). This is a result of steric repulsion which raises the energy of the stereoelectronically preferred transition-state conformation (**14**) of the aminium radical having half-vacant N_p

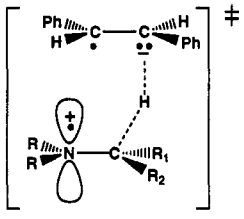

14

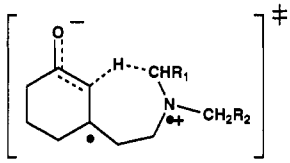

15

and filled σ_{C-H} orbital overlap. As seen by viewing the summary of Lewis' results given in Table 5, this effect is counterbalanced by the pure electronic effects (BDE effects) of α-substituents.

Different conclusions about the effects of α-substituents on tertiary aminium radical α-CH kinetic acidity have come from product distribution determinations in photochemical studies with tethered amino enones.[11] SET-promoted photoreactions of these systems follow pathways in which α-CH proton transfer occurs in intermediate zwitterionic diradicals **15**. The results of this work, included in Table 5, suggest that steric effects are less pronounced in governing kinetic acidity than in the stilbene–amine system. Moreover, the remarkable effect of the acetylene moiety on the rate of α-CH deprotonation at a propargylic center seen in the latter system was greatly attenuated in tethered enone–amine photoreactions.

(34) (a) Bordwell, F. G.; Cheng, J. P.; Bausch, M. T. *J. Am. Chem. Soc.* **1988**, *110*, 2867. (b) Zhang, X.; Bordwell, F. G. *J. Org. Chem.* **1992**, *57*, 4163. (c) Arnett, E. M.; Venimadhavan, S. *J. Am. Chem. Soc.* **1991**, *113*, 6967.

The effects of α-substituents on the rates of aminium radical α-CH deprotonation as measured by the earlier product distribution methods and by the current direct laser spectroscopic technique are reflected in the relative rate data given in Table 5. It is remarkable that the same general trends are seen in both of these data sets even though they are obtained by use of different techniques and with systems in which structurally different amine cation radicals are generated by SET to different acceptors and in which deprotonation is induced by different negatively charged bases. However, several noteworthy differences do exist. It appears that the relative α-CH deprotonation rates as judged by the stilbene–amine SET-photoaddition reactions are more sensitive to steric effects of the α-substituents (*e.g.*, compare entries a *vs* d and e). In contrast, results from the tethered amine–enone photocyclization reactions show a greater dependence of α-CH kinetic acidities on electronic contributions (BDE) of the substituents (*e.g.* compare entries a *vs* b and e). In addition, except for magnitude differences, the product distribution results agree with those from the direct laser spectroscopy results in demonstrating that the acetylene substituent has a remarkably large enhancing effect on α-CH kinetic acidities of tertiary amine cation radicals.

The differences seen in these results might be a consequence of the varying nature (*e.g.*, inter- *vs* intramolecular base pK_a and steric requirements) of the proton-transfer processes and/or the degree of C–H bond cleavage in the corresponding transitions states. For example, it is known[13] that proton transfer in the stilbene–amine photoreaction occurs in a contact ion radical pair whose rigid structure (*i.e.*, relative orientation of negative and positive radical partners) may be governed by the need for maximum charge neutralization.[35] This effect could cause kinetic acidities to more greatly weight steric factors than those determined for acetate-promoted deprotonation of free cation radical intermediates. Likewise, the intramolecular nature of proton transfer in the enone–amine zwitterionic diradicals disfavors coplanar alignment of the σ_{CH} and N_p orbitals at the cation radical center. This could very well result in the minimization of steric/stereoelectronic influences on kinetic acidity and lead to the greater importance of electronic effects of α-substituents. Clearly, α-CH deprotonation of free tertiary aminium radicals by acetate ion is not affected by these factors. Consequently, we believe that kinetic acidities of these reactive intermediates determined by the laser spectroscopic technique are more reflective of the intrinsic effects (both steric and electronic) of α-substituents.

(Silylmethyl)aniline Cation Radical Desilylation. The results described above show that the cation radical derived from the (silylmethyl)aniline **6**, like $DMA^{\bullet+}$, has a lifetime in MeCN determined only by diffusion-controlled BSET to $DCB^{\bullet-}$. Thus, in the absence of a silophile stronger than MeCN, desilylation of $\mathbf{6}^{\bullet+}$ is slow relative to BSET. However, this cation radical does participate in facile silyl-transfer reactions (eq 9) with oxygen-

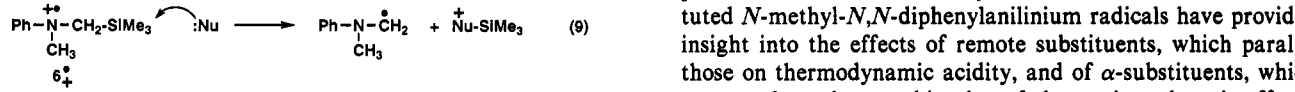

containing, nucleophilic solvents such as MeOH and H_2O. The second-order rate constants (8.9×10^5 and 1.3×10^6 M^{-1} s^{-1} (at low [H_2O]), respectively) appear to parallel silophilicity (see below).[36] In light of this it is not surprising that fluoride ion is the silophile most potent toward $\mathbf{6}^{\bullet+}$ with a second-order rate constant of 3.1×10^9 M^{-1} s^{-1} which approaches the diffusion-controlled limit in MeCN (k_{diff} = *ca.* 2×10^{10} M^{-1} s^{-1}). Thus, the high Si–F bond dissociation energy of *ca.* 200 kcal/mol (*vs* Si–O of *ca.* 135 kcal/mol) is reflected in the transition-state energetics of this silyl-transfer process.

While the observations discussed above are understandable in light of silophilicity, the effects of H_2O on $\mathbf{6}^{\bullet+}$ decay at high [H_2O] (Figure 12) are unexpected. Specifically, the contrasting behavior of $\mathbf{6}^{\bullet+}$ in MeOH–MeCN solutions (decay rates increase 20-fold in a linear fashion for [MeOH] from 2.5 to 25 M) *vs* in H_2O–MeCN solutions (decay rates increase *ca.* 7-fold in the range of [H_2O] from 2 to 5 M and remain nearly invariant with changes in [H_2O] above 5 M) is difficult to rationalize. One view of these phenomena is that two different amine cation radicals are involved in the decay process: a more reactive transient in low H_2O-content solvent systems and a more stable species at high [H_2O]. Following this reasoning, the less reactive and more reactive forms of $\mathbf{6}^{\bullet+}$ might differ in the degree of solvation by water *vs* MeCN or MeOH. An alternate explanation for these observations is based on a two-step mechanism for cation radical α-desilylation. Accordingly, this process could follow an addition–elimination route *via* the intermediacy of a reversibly formed, pentavalent silicon species (eq 10) where the degree to which the

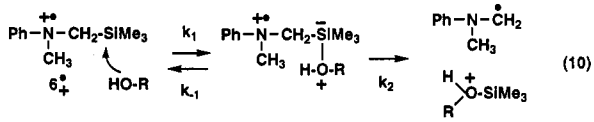

second C-Si bond breaking step contributes to the overall rate of the process is dependent on the nature of the silophile. Accordingly, the differences observed between MeOH and H_2O could be a result of the greater rate for return to the cation radical from the water ($k_{-1} > k_2$) *vs* MeOH ($k_{-1} < k_2$) bound silicate anion intermediate. In this event, the desilylation rate would remain first order in MeOH over the range of concentrations used while the process would be first order in H_2O at low concentrations and pseudo-zeroth order in H_2O at high concentrations. A definitive conclusion concerning which of these explanations best rationalizes the observations cannot be drawn at this time.

Conclusion. The investigation described above has demonstrated that laser spectroscopic techniques can be used to generate characterizable ion radical intermediates. In this fashion, a series of tertiary aminium radicals have been prepared by photoinduced SET routes as free ion radicals and solvent and salt effects on the rates of their decay by back electron transfer have been delineated. Moreover, the rates of α-desilylation and α-CH deprotonation of these transients in the presence of respective silophiles and bases can be measured by use of this methodology. Importantly, measurements by this method of the kinetic α-CH acidities of para-substituted *N,N*-dimethylanilinium radicals and α-substituted *N*-methyl-*N,N*-diphenylanilinium radicals have provided insight into the effects of remote substituents, which parallel those on thermodynamic acidity, and of α-substituents, which operate through a combination of electronic and steric effects. Finally, the results of this investigation exemplify the type of information which can be gained through a direct study of the dynamics of ion radical processes which are key in determining chemical and regiochemical selectivities of SET-promoted photochemical reactions.

Experimental Section

General Procedure. *N,N*-Dimethylaniline (**1**) (Aldrich) was distilled prior to use. The 4-methylaniline **2** (Aldrich) was used without purification. nBu_4NOAc (Aldrich) was recrystallized (EtOAc) prior to use. $nBu_4NO_2CCF_3$ was prepared by the reported procedure, as were

(35) (a) The issue of rigid orientational requirements of contact ion radical pairs has been discussed previously (ref 35b) and used in explaning the regioselectivity of an amine cation radical deprotonation reaction (ref 25b). (b) Wagner, P. J.; Kemppainen, A. E.; Jellinek, T. *J. Am. Chem. Soc.* **1972**, *94*, 7512. Wagner, P. J.; Ersfeld, D. A. *J. Am. Chem. Soc.* **1976**, *98*, 4516.

(36) Allen, A. D.; Charlton, J. C.; Eaborn, C.; Modena, G. *J. Chem. Soc.* **1957**, 3668. Allen, A. D.; Modena, G. *J. Chem. Soc.* **1957**, 3671.

(37) Clark, J. H.; Emsley, J. *J. Chem. Soc., Dalton Trans.* **1974**, *11*, 1125.

the anilines **6**,[38] **3**,[39,40] **4**,[39,40] **5**,[41] **12**,[42] **7**, **3**,[38,39] **4**,[38,39] **6**,[40] **7**,[41] **8**,[42] **9**,[41] **10**,[43], **11**,[44] **12**,[45] and **13**.[25b] The salts $LiClO_4$ (Aldrich), nBu_4NClO_4 (Fluka), nBu_4NCl (Aldrich), nBu_4NF (Aldrich), nBu_4NBF_4 (Aldrich), and $nBu_4NO_3SCF_3$ (Aldrich) were commercial materials.

Laser Flash Spectroscopy Experiments. These experiments were performed using a Questek 2120 excimer laser as the excitation source. All of the spectra and kinetic runs reported were done using XeCl reagent gas which provides UV pulses at 308 nm with a duration of 6–10 ns and a pulse energy of 30–50 mJ. Transient UV/vis absorption signals were monitored using a CW 500-W Xe lamp beam which was passed through the sample perpendicular to the excitation beam. Single-wavelength transient wave forms were digitized using a LeCroy 9420 350-MHz digital oscilloscope and transferred to a IBM PS/2 286 computer for storage and spectral analysis.

Sample solutions were placed in 10- × 10-mm quartz cuvettes which were then sealed with a rubber serum cap and purged with N_2 for 10–15 min prior to the experiment. Sample concentrations were adjusted such that their optical densities were 1.0–1.5 at the excitation wavelength.

Acknowledgment. The authors express their appreciation to the NSF (P.S.M., CHE-89-17725, and D.E.F., CHE-9119998), NIH (D.E.F., GM-45856-0181), the Italian Research Council (A.A.), and the Kyungnam National University (S.H.) for their generous financial support of this work and to Professor Ung Chan Yoon for informative discussions and helpful suggestions.

Supplementary Material Available: Figures showing transient absorption spectra and decay curves for the ion radical intermediates discussed in this paper (34 pages). This material is contained in many libraries on microfiche, immediately follows this article in the microfilm version of the journal, and can be ordered from the ACS; see any current masthead for ordering information.

(38) Gupton, J. T.; Idoux, J. P.; Baker, G.; Colon, C.; Crews, D.; Jurss, C. D.; Rampi, R. C. *J. Org. Chem.* **1983**, *48*, 2936.
(39) Fickling, M. M.; Fishcer, A.; Mann, B. R.; Packer, J.; Vaughan, J. *J. Am. Chem. Soc.* **1959**, *81*, 4226.
(40) Zhang, X. M.; Mariano, P. S. *J. Org. Chem.* **1991**, *56*, 1655.
(41) Forrest, J.; Liddell, D. A.; Horwood, T. S. *J. Chem. Soc.* **1946**, 454.
(42) Haga, K.; Oohashi, M.; Kaneko, R. *Bull. Chem. Soc. Jpn.* **1984**, *57*, 1586.
(43) Lieber, E.; Somasekhara, S. *J. Org. Chem.* **1960**, *25*, 196.
(44) Sirotkina, E. E.; Kogan, R. M.; Kovalevich, L. I.; Galkina, G. F. *Miner. Syr'e Neftekhim.* **1979**, 148. *Ref. Zh. Org. Khim.* **1980**, Abstract No. 15s171.
(45) Mostamandi, A.; Remizova, L. A.; Fomenkova, T. N.; Favorkaya, I. A. *Zh. Org. Khim.* **1982**, *18*, 848.